Surface core-level shifts on clean Si(001) and Ge(001) studied with photoelectron spectroscopy and density functional theory calculations

P. E. J. Eriksson and R. I. G. Uhrberg
Department of Physics, Chemistry and Biology, Linköping University, S-581 83 Linköping, Sweden
(Received 13 January 2010; revised manuscript received 4 March 2010; published 31 March 2010)

The Si $2p$ and Ge $3d$ core levels are investigated on the $c(4\times2)$ reconstructed surfaces of Si(001) and Ge(001), respectively. Calculated surface core-level shifts are obtained both with and without final state effects included. Significant core-level shifts are found within the four outermost atomic layers. A combination of the theoretical results and high-resolution photoemission data facilitates a detailed assignment of the atomic origins of the various components identified in the core-level spectra of both Si(001) and Ge(001).

DOI: 10.1103/PhysRevB.81.125443 PACS number(s): 79.60.Bm, 73.20.At, 71.15.−m

I. INTRODUCTION

Electrons in core states are in general not involved in the bonding in materials due to their tightly bound nature. It is instead valence electrons that form bonds and determine the electronic properties of the material. However, core electrons are still intensely studied since their localized nature, in combination with their sensitivity to the local valence charge distribution, makes them ideal for probing the chemical surrounding of individual atoms. In photoelectron spectroscopy (PES), which is the standard method for probing core states, photons are used to excite the core electrons. This photoionization induces a change in the local charge distribution; i.e., valence electrons try to screen the core hole. This redistribution can alter the energy of the emitted electron. Electrons measured by PES are thus affected both by initial state effects, i.e., the chemical surrounding of the atoms, and by final state effects, i.e., the screening by valence electrons. The importance of final state effects has been shown for metals.[1–3] In calculations performed on $p(2\times2)$ reconstructions Pehlke and Scheffler have shown[4] that also core states on the Si(001) and Ge(001) surfaces are influenced by screening. These Si $2p$ and Ge $3d$ core states have been intensely studied; see Ref. 5 and references therein. Increased energy resolution over the years has led to the identification of six[6] shifted surface components in the Si $2p$ spectrum from the $c(4\times2)$ reconstruction on Si(001). Even though the atomic origins are being debated, there is an overall agreement regarding the energy position of the major components in the Si $2p$ spectra.[6–10] The components of the Ge $3d$ spectrum from Ge(001) are less well established[11–15] due to the lack of pronounced features in the spectra.

In this paper calculated surface core-level shifts (SCLS) are used to aid in the decomposition of high-resolution Si $2p$ and Ge $3d$ core-level spectra obtained at low temperature. Calculated results with final state effects included can explain the experimentally observed SCLS quite well.

II. EXPERIMENTAL DETAILS

All PES measurements were performed at the MAX-lab synchrotron radiation facility in Lund, Sweden. Linearly polarized light from the MAX-II and MAX-III storage rings were used at beamlines I311 and I4, respectively. Si $2p$ data were acquired at I311 using a Scienta SES200 electron analyzer. The experimental energy resolution was about 30 meV and the acceptance angle was about $\pm5.5°$. The clean Si(001) sample (n-type P, 2 Ω cm) was prepared via direct resistive heating up to 1520 K until no photoemission intensity from the C $1s$ or O $1s$ core levels could be observed. Ge $3d$ data were acquired at I4 using a Specs Phoibos 100 electron analyzer. The experimental energy resolution was about 70 meV and the acceptance angle was about $\pm2°$. The clean Ge(001) sample (n-type Sb, 0.01–0.1 Ω cm) was prepared by several cycles of Ar^+ sputtering (500 eV) and heating to about 960 K.

The quality of the surface reconstructions was assessed by inspection of low-energy electron-diffraction patterns. Liquid N_2 cooling was used at both beamlines and the sample temperature was 100 K during measurements.

III. COMPUTATIONAL DETAILS

All calculated results were obtained by density functional theory calculations in the generalized gradient approximation[16] using the full-potential (linearized) augmented plane-wave+local orbitals method within the WIEN2K code.[17] The repeated slabs consisted of 11 (001)-layers. The slabs had the dimer structure of the $c(4\times2)$ reconstruction on one side and were H-terminated on the other side. A vacuum of 43 Å separated the slabs in the [001] direction. Three **k**-points were used to sample the irreducible Brillouin zone. The muffin-tin radii for the Si case were as follows: Si: 1.89 a.u.; H: 1.02 a.u. and for the Ge case, Ge: 1.93 a.u.; H: 1.04 a.u. The muffin-tin radius times the plane-wave cutoff ($R_{\mathrm{mt}}\cdot K_{\mathrm{max}}$) was 3.2. The positions of the atoms in the five top layers of the slabs were allowed to relax before the core-level calculations were performed. Calculations were also performed on symmetric slabs without H termination. These were tested with up to 19 atomic layers, but did not result in any stable core-level positions for the bulk reference layers at the center of the slab. Undesired effects of H termination have been reported in Ref. 18. When ionized atoms were present in the slab, the H layer was reported to disturb the bulk reference atoms so that all the relative SCLS would come out wrong. However, stable initial state and final state core-level shifts within layers 5–8 indicate that the slab size

 ©2010 The American Physical Society

used in this work is sufficient for obtaining a reliable bulk reference.

Initial state core-level shifts of the Si $2p$ core levels were extracted from the eigenenergies of the core states, all determined in a single calculation. The average eigenenergy of atoms in deeper layers was chosen as the reference energy for the SCLS in the initial state model. The low binding energy of the Ge $3d$ states made it difficult to treat them as core states without too much core-charge leakage. Therefore, initial state results for Ge $3d$ are not included in this paper.

Final state Si $2p$ SCLS were calculated in two ways. First the regular approach was used with the $2p$ states in the core and the individual atoms ionized and treated in individual cases. This approach was not possible in the case of Ge due to the low binding energy of Ge $3d$. Instead, final state core-level shifts were calculated using a two window semicore approach[19] where again each of the atoms was treated in individual cases. In a first step, one electron was removed from the $2p$ $(3d)$ core states of one atom in the case of Si (Ge). As a result, the $2p$ $(3d)$ states of that atom were shifted to a slightly higher binding energy. Next, the cutoff energy that separates the core states from the valence states was decreased so that all the $2p$ $(3d)$ states were treated as valence states. In order to keep the $2p$ $(3d)$ states of only one atom ionized, a two window semicore calculation was finally utilized. The energy position separating the two windows was chosen between the downshifted $2p$ $(3d)$ states and the $2p$ $(3d)$ states of the other atoms. In the window with the downshifted $2p$ $(3d)$ states the occupation number was one electron short. The other window contained the fully occupied $2p$ $(3d)$ states of all other atoms. A background charge was added to compensate for the removed electron. The two window approach appears to be reliable, since in the Si case the two methods used, i.e., Si $2p$ in the core and the two window approach, resulted in final state SCLS which differ by at most ± 0.03 eV. Total energies were higher when core holes were introduced compared to the nonionized case. The average total energy when atoms in deeper layers were ionized was chosen as the reference energy, and the SCLS are the total energy deviations from this reference value that arise when different atoms closer to the surface were ionized.

IV. RESULTS AND DISCUSSION

A. Core-level shift calculations

The calculations were performed on $c(4\times 2)$ reconstructions of Si(001) and Ge(001) as shown in Fig. 1. Atomic

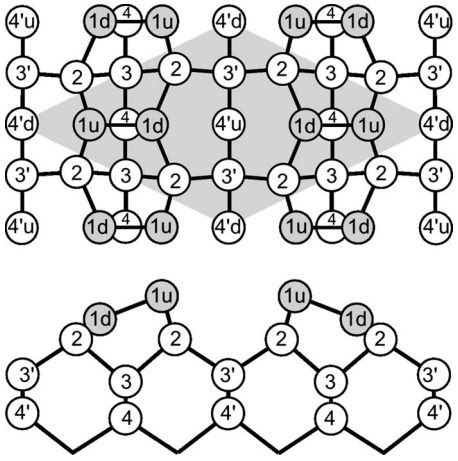

FIG. 1. Top and side views of the $c(4\times 2)$ reconstruction.

labels in the four top layers were adopted from Ref. 20 and were used for both Si and Ge. In the relaxed Si structure we obtained a dimer bond length and a tilt angle of 2.36 Å and 18.95°, respectively. An earlier calculation using the $c(4\times 2)$ unit cell resulted in values of 2.29 Å and 17.5° (Ref. 21). In Refs. 20 and 22, the tilt angle was found to be 19°. Our calculations in the Ge case gave a dimer bond length and a tilt angle of 2.56 Å and 20.78°, respectively. Corresponding values from the literature include 2.51 Å and 19.5° (Ref. 23), 2.50 Å and a quite small tilt angle of 15.5° (Ref. 24), and finally 19.1° for the tilt angle in Ref. 22. Overall, the present values are in line with the majority of previous publications.

Si $2p$ SCLS were calculated in both the initial and the final state picture. Due to the computational difficulties mentioned in Sec. III, only final state results are included for Ge $3d$. The results of our calculations are summarized in Table I. In layers 5–8 the variation in energy position was very small and the average value was chosen as the bulk reference. Core-level energies of atoms in the three layers closest to the H termination deviate from this bulk value and data from these layers were not used.

The change in relative binding energy when screening was included is given as Δ for Si $2p$ in Table I. The results from the calculations are also illustrated in Fig. 2. The dimer down-atom $(1d)$ is most affected by the screening. This has been attributed to the polarization of the tilted dimers.[4] In the nonionized case, charge transfer within the dimers results in an unoccupied state mainly localized at the down-atom; see

TABLE I. Surface core-level shifts of the atoms in the $c(4\times 2)$ reconstruction on Si(001) and Ge(001) calculated in the initial and final state picture (Si $2p$) and final state picture (Ge $3d$). Δ is the difference in relative shift between initial and final state cases. All values are given in eV. Atomic labels are from Fig. 1 and the superscripts indicate the number of times each atom appears in the $c(4\times 2)$ unit cell.

Atom		$1u^2$	$1d^2$	2^4	3^2	$3'^2$	4^2	$4'u^1$	$4'd^1$
Si	Initial	−0.35	0.51	0.08	−0.01	0.22	−0.19	0.19	0.09
	Final	−0.49	0.10	0.00	−0.11	0.24	−0.26	0.19	0.10
	Δ	−0.14	−0.40	−0.08	−0.10	0.02	−0.07	−0.00	0.01
Ge	Final	−0.51	−0.10	−0.23	−0.21	−0.00	−0.15	−0.01	−0.06

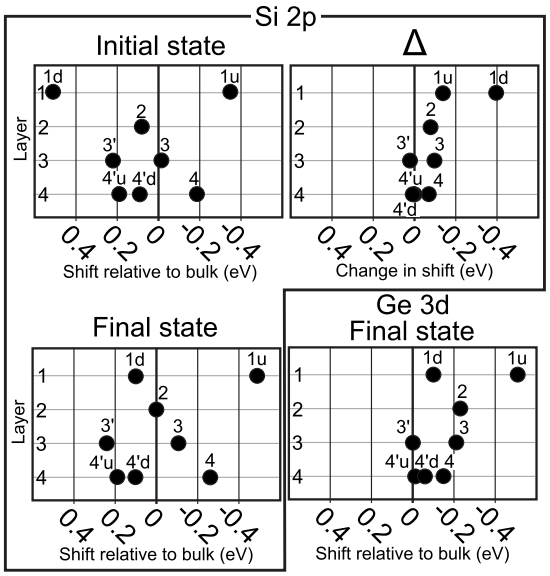

FIG. 2. Binding energy diagrams of the calculated SCLS in Table I. For Si 2*p*, initial state and final state SCLS are given. Δ is the difference between final state and initial state results for Si 2*p* and it indicates the effect of screening on the relative binding energy. For Ge 3*d*, only final state SCLS are given.

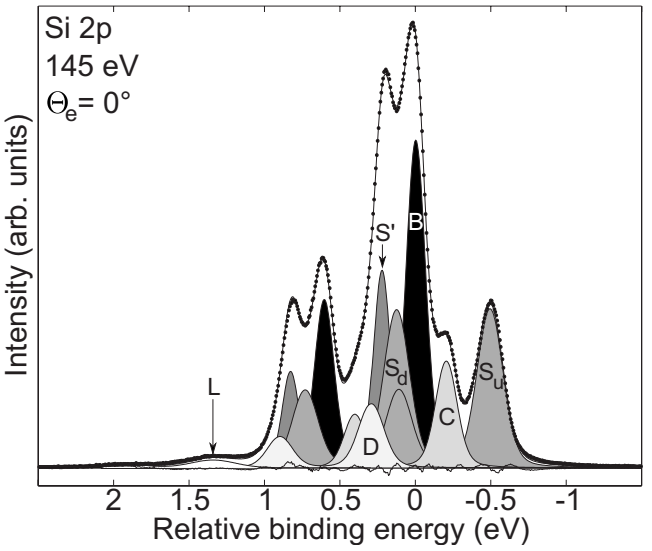

FIG. 3. Normal emission Si 2*p* core-level spectrum (dots) obtained at 100 K. A bulk (black) and six shifted surface components (gray), constructed of spin-orbit split Voigt functions, are used to generate the fit (solid curve). The residual intensity is shown relative to the base line. An integrated background has been subtracted beforehand. All fitting parameters are given in Table II.

Ref. 4. The unoccupied state is shifted down below the Fermi level upon ionization of the dimer down-atom. The resulting localized increase in electron density provides efficient screening of the core holes at the down-atom. A more negative Δ for atoms near the surface compared to deeper atoms and the fact that atoms under the dimer rows are more affected by the screening compared to atoms between the dimer rows are consistent with the observations in Ref. 4. The atoms between the dimer rows, $3'$, $4'u$, and $4'd$, appear to have positive Δ; i.e., they are slightly less affected by screening compared to the bulk reference atoms.

Si 2*p* SCLS in the initial state model are qualitatively in line with Ref. 4. Our final state results, however, are different both qualitatively and quantitatively regarding atoms 1*d* and 2. In Ref. 4, atom 1*d* showed a negative relative shift while that of atom 2 was positive. The signs of the SCLS of these two atoms, as obtained in this study, are opposite to Ref. 4. Our final state results for Si 2*p* are, on the other hand, in nice agreement with the more recent results in Ref. 20.

Regarding the Ge(001) case, the only calculated Ge 3*d* SCLS are those obtained on a Ge(001) $p(2\times2)$ structure in Ref. 4. The calculated shifts indicated an overestimation of the screening compared to experiment.[13] As will be shown below the Ge 3*d* results presented in this paper (Table I) are in better agreement with experiments.

B. Si 2*p*

The decomposition of the Si 2*p* core-level spectra has resulted in the identification of several shifted surface-related components. The generally accepted decomposition, originating from Ref. 7, consists of five shifted components in addition to a bulk component. A decomposition where these five surface shifted components and a bulk component are used is shown in Fig. 3. In addition, a weak component *L* was found on the high binding energy tail of the spectrum in agreement with Ref. 6. The fitting parameters of the bulk and the six shifted components are given in Table II.

The clearly separated S_u component has been established as originating from the up-atom of the tilted dimer. It is found at −0.49 eV in the fit as well as in the calculated final state results. The dimer down-atom component, S_d, is positioned at 0.13 eV in the fit, which is a slightly larger value than in Ref. 7 (0.06 eV), but within the range (0.03–0.13 eV) suggested in Ref. 6. This shift is close to the 0.10 eV that 1*d* exhibits in the final state calculations. In the initial state calculation the 1*d* component is at 0.51 eV. This is clearly not in agreement with the PES data. In the discussion below, only final state data are therefore included. Based on the calculated shifts, atom $4'd$ is also expected to contribute to the spectrum at the energy of the dimer down-atom. A relatively strong bulk component, *B*, is also consistent with the calculations even though the surface sensitivity is very high at a photon energy of 145 eV (~40 eV electron kinetic energy). The calculated shift corresponding to the second layer atoms is close to zero and these atoms (1 ML) will therefore contribute strongly to the intensity at the position of the bulk component. The *C* component can be explained by the calculated shift of atom 4. The strong intensity of *C*, nearly half of S_u, suggests that also atom 3 contributes. An origin in these deeper layers is supported by more surface sensitive spectra taken with a 60° emission angle, where the relative intensity of *C* is reduced. The energy position of the S' component is consistent with atoms $3'$ and $4'u$. The very weak *L* component at 1.34 eV cannot be explained by the calculations. It has been attributed to a loss process via an interband transition between surface bands.[6]

The presence of a *D* component has been reported before,[6,9] but no explanation has so far been published. The

TABLE II. Fitting parameters of the Si $2p$ components in Fig. 3. The parameters are binding energy relative to the bulk (E), Gaussian width (GW), and percentage (%) of the total intensity. The Lorentzian width was 0.046 eV. The spin-orbit split was 0.605 eV and the branching ratios were in the range 0.488–0.511. The last two rows, labeled "Origins," summarize the identification of the atomic origins of the various components. The number that appears as a subscript on the atom label is the calculated core-level shift.

	L	D	S'	S_d	B	C	S_u
E (eV)	1.34	0.30	0.22	0.13	0	−0.22	−0.49
GW (eV)	0.33	0.17	0.11	0.18	0.13	0.14	0.18
%	1.5	7.2	15.4	18	29.4	10.4	18.1
Origins			$3'_{0.24}$	$1d_{0.10}$	$\mathrm{Bulk}_{0.00}$	$4_{-0.26}$	$1u_{-0.49}$
			$4'u_{0.19}$	$4'd_{0.10}$	$2_{0.00}$	$(3_{-0.11})$	

intensity of D is quite weak. It varies between about 4% and 7% depending on the position of the other components. PES data taken with 0° and 60° emission angles indicate that it originates from the surface. Since screening tends to shift the surface components toward lower binding energy, one could argue that incomplete screening of the $1d$ atoms may, due to defects, result in a shifted component at the energy position of D. However, a comparison of the relative intensities of D and $1d$ suggests that the D component would correspond to about 0.1–0.2 ML or 20%–40% of the $1d$ atoms. This is far too high for such an explanation to be likely considering the quality of the clean Si(001) surface.

The identified origins of the components are given in the last two rows in Table II. Considering the nice agreement in energy position between most experimentally obtained components and the calculated shifts, it is likely that the unidentified D and L components are induced by some surface features not treated in the calculations. Experimentally obtained relative intensities are in qualitative agreement with what can be expected from a simple layer attenuation model applied to the calculated components.

C. Ge 3*d*

The atomic structure of Ge(001) $c(4\times2)$ is very similar to that of Si(001) $c(4\times2)$. Also the PES data on the Ge $3d$ core level show similarities to Si $2p$ data. However, the Ge $3d$ core-level spectra show significantly less features than Si $2p$ spectra. This appears to be an intrinsic property of Ge $3d$, since pushing the experimental resolution of state-of-the-art equipment only results in sharper spectra to some limited degree. As a consequence of the lack of distinct features it is difficult to decompose the Ge(001) Ge $3d$ core-level spectra based on experimental data only.

The dotted curves in Fig. 4 show a Ge $3d$ core-level spectrum recorded using a photon energy of 85 eV (~50 eV electron kinetic energy) and 60° emission angle resulting in enhanced surface sensitivity. Despite this, the only apparent feature is a peak on the low binding energy side. Similar to Si $2p$ this feature has in earlier studies[11–13,15] been attributed to the dimer up-atom. The bulging shape on the right side of the main peak suggests that there are components hidden on the low binding energy side. The binding energy of the dimer up-atom component relative to the bulk reference is not well established experimentally. Values range from −0.43 to −0.56 eV in Refs. 11–13. Compared to these earlier papers, the up-atom component in Fig. 4 is much better resolved. That, in combination with the calculated SCLS, facilitates a more detailed decomposition of the Ge $3d$ spectrum. The cal-

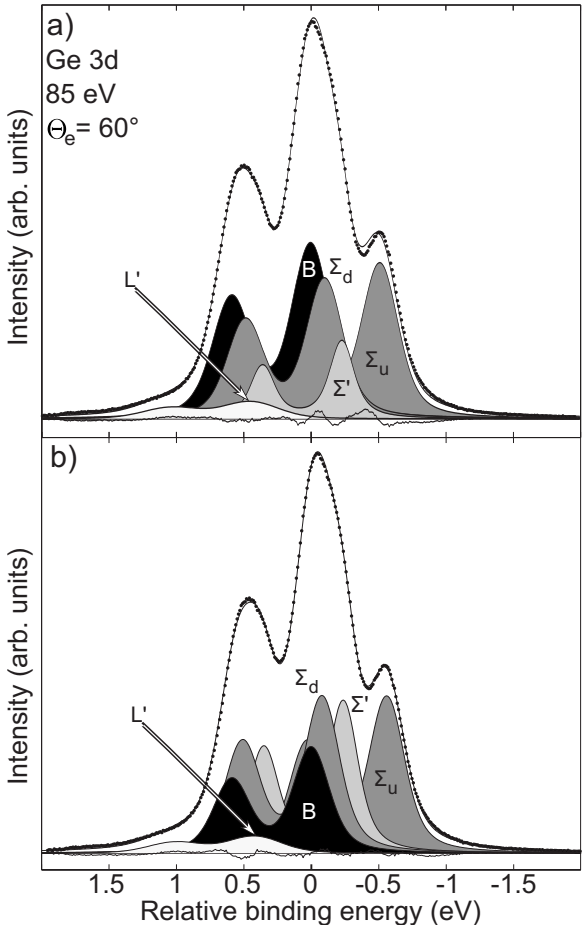

FIG. 4. 60° emission angle Ge $3d$ core-level spectrum (dots) obtained at 100 K. A bulk (black) and four shifted surface components (gray) constructed of spin-orbit split Voigt functions are used to generate the fit (solid curve). In (a), constraints from calculated results in Table I are used on the fitting parameters. In (b), the constraints have been relaxed. The residual intensity is shown relative to the base line. An integrated background has been subtracted beforehand. Fitting parameters are given in Table III.

TABLE III. Fitting parameters of the Ge 3*d* components in Fig. 4. The parameters are binding energy relative to the bulk (*E*), Gaussian width (GW) and percentage (%) of the total intensity. The Lorentzian width was 0.15 eV and the spin-orbit split was 0.59 eV. The branching ratios were in the range 0.649–0.707. The last three rows, labeled "Origins," summarize the identification of the atomic origins of the various components. The number that appears as a subscript on the atom label is the calculated core-level shift.

		L'	B	Σ_d	Σ'	Σ_u
Figure 4(a)	E (eV)	0.45	0	−0.10	−0.23	−0.51
	GW (eV)	0.41	0.26	0.24	0.12	0.24
	%	4.4	30.7	25.2	10.2	27.8
Figure 4(b)	E (eV)	0.42	0	−0.08	−0.24	−0.56
	GW (eV)	0.39	0.23	0.22	0.17	0.22
	%	4.1	18.7	27.2	22.9	27.1
Origins			$\text{Bulk}_{0.00}$	$1d_{-0.10}$	$2_{-0.23}$	$1u_{-0.51}$
			$3'_{-0.00}$	$4'd_{-0.06}$	$3_{-0.21}$	
			$4'u_{-0.01}$	$(4_{-0.15})$		

culated Ge 3*d* SCLS in Table I are all negative, of which some are very close to zero. This indicates a qualitative agreement between the general appearance of the spectrum and the calculations. The fitting result using the theoretically derived shifts of Σ_u and Σ_d, i.e., the shifts corresponding to atoms $1u$ and $1d$, is shown in Fig. 4(a). Four shifted components, Σ_u, Σ_d, Σ', and L', in addition to the bulk component, B, were necessary. The fitting parameters are given in Table III. Contrary to Refs. 14 and 15, we find no evidence of any surface component shifted to the left of the main peak. Several constraints were used in the fit. The intensity of the dimer down-atom component Σ_d should be similar to the up-atom component Σ_u. Since the shifts of Σ_d and Σ_u relative to the bulk component were fixed to the calculated values, there was a relatively large residual intensity. The Σ' component on the low binding energy side was added to take care of most of that. Although the quality of the resulting fit is questionable, it gives a hint on the plausibility of the parameters used. The extra component, Σ', at −0.23 eV should, even if the calculations are only qualitatively correct, originate from atoms 2, 3, and possibly also 4; see Fig. 2. However, Σ' in Fig. 4(a) is too weak to account for those atoms. Furthermore, the Gaussian width of 0.12 eV is too small to be realistic considering that the other components are at least twice as broad.

Relaxed constraints are clearly necessary to obtain both an improved fit and a more physically sound Σ' component. In Fig. 4(b) the same spectrum has been fitted using slightly different parameters; see Table III. Σ_u and Σ_d have moved apart and Σ', which is located in between, has gained intensity. Σ_u is shifted by −0.56 eV, i.e., the same value as in Ref. 12. In that paper, a second surface component, in addition to the dimer up-atom component, at −0.24 eV was used in the fit. This is consistent with Σ', also positioned at −0.24 eV. The atomic origins of the components used to fit the Ge 3*d* spectrum are summarized in the three bottom rows of Table III. There is a quite nice agreement and it is only atom 4 that does not fit with any of the components. However, the intensity may be expected to be weak from atom 4 since it is a fourth layer atom residing underneath the dimer rows and constituting 0.5 ML.

The calculations in Ref. 4 found the $1d$, $1u$, and second layer components at −0.39, −0.67, and −0.16 eV, respectively; i.e., the second layer component exhibited a higher relative binding energy than $1d$, which is opposite to the results presented in Fig. 2. Based on the results from Ref. 4, the Σ' and Σ_d labels in Fig. 4(b) would swap places. Judging from the similarity in the intensities of Σ_d and Σ' in Fig. 4(b), such an interpretation would be equally valid. However, the final state SCLS of the dimer atoms in Ref. 4 are quantitatively not in agreement with the PES data. The results in Table I do not indicate any overestimation of the screening effect as discussed in Ref. 4. The −0.51 eV shift of $1u$ is close to the experimental value but significantly smaller than the shift reported in Ref. 4. Thus, the present results should provide a better description of the experimental data.

V. SUMMARY

In this paper we have shown that calculated surface core-level shifts in the final state picture of both Si(001) and Ge(001) agree closely with experimental results obtained by core-level spectroscopy. The combination of theoretical and experimental results allowed for an unprecedented detailed assignment of the atomic origins of the various components that constitute the core-level spectra. The identification of the atomic origins could be carried out successfully as deep as the fourth atomic layer. The four topmost layers contain eight inequivalent groups of Si (Ge) atoms and a positive assignment could be made for seven of them in both the Si and Ge cases.

ACKNOWLEDGMENTS

This work was financially supported by the Swedish Research Council. The calculations were performed on the Neolith cluster at the National Supercomputer Centre in Linköping, Sweden.

[1] B. Johansson and N. Mårtensson, Phys. Rev. B **21**, 4427 (1980).
[2] M. Aldén, I. A. Abrikosov, B. Johansson, N. M. Rosengaard, and H. L. Skriver, Phys. Rev. B **50**, 5131 (1994).
[3] I. A. Abrikosov, W. Olovsson, and B. Johansson, Phys. Rev. Lett. **87**, 176403 (2001).
[4] E. Pehlke and M. Scheffler, Phys. Rev. Lett. **71**, 2338 (1993).
[5] M. V. Gomoyunova and I. I. Pronin, Tech. Phys. **49**, 1249 (2004).
[6] H. Koh, J. W. Kim, W. H. Choi, and H. W. Yeom, Phys. Rev. B **67**, 073306 (2003).
[7] E. Landemark, C. J. Karlsson, Y.-C. Chao, and R. I. G. Uhrberg, Phys. Rev. Lett. **69**, 1588 (1992).
[8] P. De Padova, R. Larciprete, C. Quaresima, C. Ottaviani, B. Ressel, and P. Perfetti, Phys. Rev. Lett. **81**, 2320 (1998).
[9] R. I. G. Uhrberg, J. Phys.: Condens. Matter **13**, 11181 (2001).
[10] Y. Yamashita, S.-I. Machida, M. Nagao, S. Yamamoto, Y. Kakefuda, K. Mukai, and J. Yoshinobu, Jpn. J. Appl. Phys., Part 2 **41**, L272 (2002).
[11] R. D. Schnell, F. J. Himpsel, A. Bogen, D. Rieger, and W. Steinmann, Phys. Rev. B **32**, 8052 (1985).
[12] G. Le Lay, J. Kanski, P. O. Nilsson, U. O. Karlsson, and K. Hricovini, Phys. Rev. B **45**, 6692 (1992).
[13] E. Landemark, C. J. Karlsson, L. S. O. Johansson, and R. I. G. Uhrberg, Phys. Rev. B **49**, 16523 (1994).
[14] A. Goldoni, S. Modesti, V. R. Dhanak, M. Sancrotti, and A. Santoni, Phys. Rev. B **54**, 11340 (1996).
[15] T.-W. Pi, J.-F. Wen, C.-P. Ouyang, and R.-T. Wu, Phys. Rev. B **63**, 153310 (2001).
[16] J. P. Perdew, K. Burke, and M. Ernzerhof, Phys. Rev. Lett. **77**, 3865 (1996).
[17] P. Blaha, K. Schwarz, G. K. H. Madsen, D. Kvasnicka, and J. Luitz, *WIEN2K, An Augmented Plane Wave+Local Orbitals Program for Calculating Crystal Properties* (Karlheinz Schwarz, Tech. Universität Wien, Austria, 2001).
[18] M. P. J. Punkkinen, K. Kokko, L. Vitos, P. Laukkanen, E. Airiskallio, M. Ropo, M. Ahola-Tuomi, M. Kuzmin, I. J. Väyrynen, and B. Johansson, Phys. Rev. B **77**, 245302 (2008).
[19] *Plane waves, Pseudopotentials, and the LAPW Method*, 2nd ed., edited by D. J. Singh and L. Nordström (Springer-Verlag, Berlin, 2006), p. 84.
[20] O. V. Yazyev and A. Pasquarello, Phys. Rev. Lett. **96**, 157601 (2006).
[21] J. E. Northrup, Phys. Rev. B **47**, 10032 (1993).
[22] J. Nakamura and A. Natori, Jpn. J. Appl. Phys. **44**, 5413 (2005).
[23] Y. Yoshimoto, Y. Nakamura, H. Kawai, M. Tsukada, and M. Nakayama, Phys. Rev. B **61**, 1965 (2000).
[24] L. Spiess, A. J. Freeman, and P. Soukiassian, Phys. Rev. B **50**, 2249 (1994).